Published in final edited form as:
J Porphyr Phthalocyanines. 2010 January 1; 14(1): 115–122. doi:10.1142/S1088424610001714.

Inter-Ring Interactions in [Fe(TalkylP)(Cl)] (alkyl = ethyl, *n*-propyl, *n*-hexyl) Complexes: Control by *meso*-Substituted Groups

Ming Li[†], **Teresa J. Neal**[†], **Noelle Ehlinger**[†], **Charles E. Schulz**[‡], and **W. Robert Scheidt**[†]

[†]The Department of Chemistry and Biochemistry, University of Notre Dame, Notre Dame, Indiana 46556

[‡]The Department of Physics, Knox College, Galesburg, Illinois 61401

Abstract

Syntheses, molecular structures and magnetic susceptibilities of three *meso*-substituted high-spin iron(III) porphyrinate complexes ([Fe(TEtP)(Cl)], [Fe(TPrP)(Cl)], and [Fe(THexP)(Cl)]) are described. It was determined that the inter-ring interactions within each dimeric unit change upon alteration of the alkyl groups at the meso-positions. Magnetic exchange couplings between iron centers of the dimers are in accord with the trends in structural inter-ring geometries. Crystal data for [Fe(TEtP)(Cl)]: a = 10.1710(5) Å, b = 11.309(3) Å, c = 12.170(3) Å, α = 91.774(9) °, β = 113.170 (14) °, γ = 112.149(9) °, V = 1165.2(4) Å^3, triclinic, $P\bar{1}$, Z = 2, R_1 = 0.0844 and ωR_2 = 0.2073 for observed data. Crystal data for [Fe([Fe(TPrP)(Cl)])(Cl)]: a = 13.040(2) Å, b = 15.221(2) Å, c = 14.6681(9) Å, β = 109.997(11) °, V = 2735.9(7) Å^3, monoclinic, $P2_1/n$, Z = 4, R_1 = 0.0477 and ωR_2 = 0.1176 for observed data. Crystal data for [Fe(THexP)(Cl)]: a = 10.246(7) Å, b = 12.834(4) Å, c = 17.420(15) Å, α = 69.74(3) °, β = 87.52(4) °, γ, = 84.89(3) °, V = 2140(2) Å^3, triclinic, $P\bar{1}$, Z = 2, R_1 = 0.1024 and ωR_2 = 0.2659 for observed data.

Keywords

iron(III)*meso*-tetraalkylporphinates; inter-ring interaction; magnetic exchange couplings; Crystal Structures

Introduction

It is well-known that π–π interactions between two or more porphyrin molecules in close proximity are present in photosynthetic proteins, including light-harvesting chlorophyll arrays [1] and the photosynthetic reaction center special pair.[2] The interactions have played a critical role in electron(or energy)-transfer process in photosynthetic proteins. Scheidt and Lee[3] surveyed the inter-ring geometry for all structurally characterized neutral porphyrin dimers. They noted that the observed lateral shifts tend to cluster around specific values rather than displaying a continuous distribution. It has been shown that such dimerizations have a strong effect on the chemical reactivity and spectroscopic properties of the porphyrinato complexes. [4]–[6]

Correspondence to: Charles E. Schulz; W. Robert Scheidt.

Supporting Information Available. The CIF files for the crystal structures were deposited at the CCDC. The CCDC deposition numbers of [Fe(TEtP)(Cl)], [Fe(TPrP)(Cl)], and [Fe(THexP)(Cl)] are 744649, 744651 and 744650, respectively. These data can be obtained free of charge from The Cambridge Crystallographic Data Centre via www.ccdc.cam.ac.uk/data_request/cif.

Studies on the replacement of *meso*-aryl substituents in metallotetrarylporphyrins by alkyl groups have attracted much attention recently owing to the fact that the alkyl-substituents may profoundly inuence the molecular and electronic structure as well as catalytic properties of the resulting complexes.[7]–[28] In the present work, we describe the synthesis and characterization of a series of *meso*-(tetraalkylporphinato)iron(III) chloride complexes. Their molecular structures indicate that inter-ring interactions change with alteration of the alkyl group substitutions in the *meso* positions. Also, we have investigated the effect of such inter-ring interaction on magnetic exchange interactions between the iron centers of these *meso*-alkyl substituted porphyrinates.

Experimental Section

General Information

Dichloromethane was distilled over potassium carbonate and hexanes were distilled over sodium benzophenone. All other chemicals were used as received from Aldrich or Fisher. *meso*-Tetra-*n*-propylporphyrin (H_2TPrP) was prepared according to Neya's method,[29] while *meso*-tetraethylporphyrin (H_2TEtP) and *meso*-tetra-*n*-hexylporphyrin (H_2THexP) was prepared according to Lindsey's method.[30] Iron was inserted into the three H_2-*meso*-tetraalkylporphyrinato derivatives by standard methods.[31] UV-vis spectra were recorded on a Perkin-Elmer Lambda 19 spectrometer and IR spectra on a Perkin-Elmer model 883 as KBr pellets. EPR spectra were obtained at 77 K on a Varian E-12 spectrometer operating at X-band.

Structure Determinations

Single crystals of [Fe(TPrP)(Cl)][32] and [Fe(TEtP)(Cl)] were obtained by slow di_usion of hexanes into a CH_2Cl_2 solution of the metalloporphyrin, whereas single crystals of [Fe(THexP)(Cl)] were obtained by slow evaporation of a concentrated CH_2Cl_2 solution. X-ray diffraction data for all the complexes were collected on a Nonius FAST area-detector diffractometer with a Mo rotating anode source ($\bar{\lambda}$ = 0.71073 Å). Our detailed methods and procedure for small molecule X-ray data collection have been described previously.[33]

The structure of [Fe(TPrP)(Cl)] was solved by Patterson methods, while [Fe(TEtP)(Cl)] and [Fe(THexP)(Cl)] were solved by direct methods.[34] All remaining non-hydrogen atoms were located by difference Fourier synthesis. The structures were refined against F^2 using the program SHELXL-93,[35] in which all data collected were used including negative intensities. Hydrogen atoms of the porphyrin ligands and the solvent molecule were idealized with the standard SHELXL-93 idealization methods. A modified[36] version of the absorption correction program DIFABS and extinction were applied for [Fe(TEtP)(Cl)] and [Fe(THexP)(Cl)]. For [Fe(THexP)(Cl)], it was found that three hexyl substituents were disordered. One hexyl chain is disordered over two half-occupied positions (C(80) to C(85) and C(90) to C(95)). The last three carbon atoms of another hexyl group are disordered; C(4) to C(6) have refined occupancies of 0.76, while C(41) to C(61) have occupancies of 0.24. In the third disordered hexyl group, the final methyl group is disordered over two positions (C(24) and C(240)) with refined occupation factors of 0.63 and 0.37, respectively. There is one dichloromethane molecule with an occupancy factor of 0.10. Brief crystallographic data for all three complexes are listed in Table 1. Complete crystallographic details are available from the CCDC (Supporting Information).

Magnetic Susceptibility Measurements

Magnetic susceptibility measurements were obtained on ground samples (immobilized in Dow Corning silicone grease) in the solid state over the temperature range 6–300 K on a Quantum Design MPMS SQUID susceptometer. Measurements at two fields (2 and 20 kG) showed that no ferromagnetic impurities were present and that preferential orientation of unpaired spins

was not taking place. χ_M was corrected for the underlying porphyrin ligand diamagnetism according to previous experimentally observed values;[38] all remaining diamagnetic contributions (χ_{dia}) were calculated using Pascal's constants.[39];[40] All measurements included a correction for the diamagnetic sample holder and the diamagnetic silicone grease.

Results

The molecular structures of three meso alkyl-substituted (chloro)iron(III) porphyrinate derivatives have been determined. The three iron porphyrin complexes differ in the length of the alkyl side chains with *meso*-substituents of ethyl, [Fe(TEtP)(Cl)], *n*-propyl, [Fe(TPrP)(Cl)], and *n*-hexyl, [Fe(THexP)(Cl)]. A labeled ORTEP diagram of [Fe(TPrP)(Cl)] is shown in Figure 1. Labeled ORTEP diagrams of [Fe(TEtP)(Cl)] and [Fe(THexP)(Cl)] can be found in Figure 2 and Figure 3. Table 1 details selected crystallographic details for all three complexes.

Bond distances and bond angles around the iron(III) atom in the three derivatives are listed in Table 2. Figure 4a–c presents formal diagrams of the porphinato cores in [Fe(TEtP)(Cl)], [Fe (TPrP)(Cl)], and [Fe(THexP)(Cl)], respectively, displaying the perpendicular displacements of each atom from the 24-atom mean plane of the porphinato core. Figure 4 also contains the average bond lengths and bond angles (including standard deviations) for each complex. The porphyrin core of [Fe(TEtP)(Cl)] (Figure 4a) is planar, while the porphyrin cores of [Fe(TPrP) (Cl)] and [Fe(THexP)(Cl)] are S_4– ruffled (Figures 4b and 4c).

Solid-state π–π dimer formation is seen in all three [Fe(TalkylP)(Cl)] complexes. Figure 5a–c shows edge-views and top-views of the closest interacting pair of porphyrin dimers for [Fe (TEtP)(Cl)], [Fe(TPrP)(Cl)], and [Fe(THexP)(Cl)], respectively. The inter-ring geometries for each dimer, including Fe…Fe and Ct…Ct distances, lateral shifts (L.S.), and mean plane separations (M.P.S.), are summarized in Table 3.

Temperature-dependent magnetic susceptibility measurements were carried out on the [Fe (TEtP)(Cl)] and [Fe(TPrP)(Cl)] complexes over the temperature range 6–300 K. Figure 6 shows the temperature-dependent magnetic moments for both complexes.

Discussion

Crystal Structures

The general trends in bond lengths and bond angles for all three [Fe(TalkylP)(Cl)] complexes are similar to those found in [Fe(TPP)(Cl)][41] and [Fe(OEP)(Cl)].[42] The coordination geometry of the iron centers in the [Fe(TalkylP)(Cl)] complexes is characteristic of high-spin iron(III) porphyrins. The equatorial Fe–N_p bond lengths in [Fe(TEtP)(Cl)], [Fe(TPrP)(Cl)], and [Fe(THexP)(Cl)] (2.053(5) Å, 2.058(8) Å, and 2.060(6) Å, respectively) fit nicely into the category of typical high-spin Fe–N distances (≥ 2.045 Å).[43] A close inspection of bond angles reveals significant differences in the Fe–N–C(a) angles when comparing [Fe(TEtP)(Cl)] to [Fe ([Fe(TPrP)(Cl)] and [Fe(THexP)(Cl)] (Figure 4). In [Fe(TEtP)(Cl)], the two types of Fe–N–C (a) angles are nearly equivalent [126.5(2) ° and 125.7(4) °] and are similar to those found in [Fe(TPP)(Cl)][41] [126.9(8) ° and 125.8(6) °] and [Fe(OEP)(Cl)][42] [126.3(6) ° and 126.5 (5)°]. In contrast, [Fe(TPrP)(Cl)] and [Fe(THexP)(Cl)] have two distinct types of Fe–N–C(a) angles with one of the angles being larger than the other [128.1(2) ° and 124.5(7) ° for [Fe (TPrP)(Cl)] and 127.4(2) ° and 124.9(3)° for [Fe(THexP)(Cl)]]. The differences in Fe–N–C(a) angles are apparently the result of the change in macrocyclic conformations among these complexes. In [Fe(TEtP)(Cl)], the macrocycle is basically planar, as evidenced by an average deviation of the macrocycle carbon atoms from the 24-atom mean plane of 0.03 Å, and a maximum displacement of 0.06 Å (Figure 4a). The macrocycles of [Fe(TPrP(Cl)] and [Fe (THexP)(Cl)] are ruffled to reduce steric interactions between the *meso*-alkyl and neighboring

pyrrole groups. The average and maximum deviations of the macrocycle carbon atoms from the 24-atom mean plane of [Fe(TPrP)(Cl)] and [Fe(THexP)(Cl)] are 0.18 Å and 0.38 Å, and 0.15 Å and 0.33Å, respectively. Thus, ruffling of the macrocycles of [Fe(TPrP)(Cl)] and [Fe(THexP)(Cl)] contributes to the significant differences in Fe–N–C(a) angles found in these two complexes. The effects of ring ruffling are also reflected in the coordination environment of the iron centers; the out-of-plane displacement of the Fe atom in planar [Fe(TEtP)(Cl)] (0.48 Å) is slightly smaller than those found in ruffled [Fe(TPrP)(Cl)] and [Fe(THexP)(Cl)] (0.57 Å and 0.55 Å, respectively). Additionally, compared to planar [Fe(TEtP)(Cl)], an increase of the Fe–N_p distances accompanied by a decrease of the Fe–Cl bond lengths is observed in ruffled [Fe(TPrP)(Cl)] and [Fe(THexP)(Cl)] (*see* Table 2).

In addition to the differences in ring conformations, the inter-ring interactions among the [Fe(TalkylP)(Cl)] dimers are dramatically different. The lateral shift values increase from ethyl to hexyl groups (Table 3). The lateral shift of [Fe(TEtP)(Cl)] is 3.79 Å, which falls into the intermediate (I) group, as defined by Scheidt and Lee,[3] whereas the dimeric units of [Fe(TPrP)(Cl)] and [Fe(THexP)(Cl)] show weaker interactions (Group W) with larger lateral shifts (4.29Å and 4.48 Å, respectively). The differences in lateral shifts among these complexes can be attributed to the orientation of the *meso*-substituents of the porphyrin rings. Each porphyrin in [Fe(TEtP)(Cl)] has two ethyl groups pointing up and two pointing down in an orientation as to favor inter-ring overlap. However, [Fe(TPrP)(Cl)] and [Fe(THexP)(Cl)] have alternating up and down *meso*-substituents which leads to less favorable inter-ring overlap.

Magnetic Susceptibility Measurements

Temperature-dependent magnetic susceptibility measurements were carried out on [Fe(TEtP)(Cl)] and [Fe(TPrP)(Cl)] to investigate the differences in magnetic exchange between the high-spin iron(III) metal centers of these porphyrinate dimers. To date, high-spin ferric porphyrin complexes have been thoroughly investigated by using physical techniques such as EPR, Mössbauer, and NMR; however, relatively few detailed and accurate magnetic susceptibility measurements of high-spin mononuclear iron(III) porphyrins have been carried out over a wide range of temperatures. For example, magnetization studies of ferric tetraphenylporphyrins were carried out at field strengths of up to 50 kG but were only studied between a narrow temperature range (2–20 K).[44] Original magnetic susceptibility data for [Fe(OEP)(Cl)][42] were reported at only a few temperatures and showed large scatter; recently, more accurate data for this compound has been reported from 4–100 K.[46] Although it is the lower temperature region that is most informative concerning the magnitude of the magnetic exchange interaction, large temperature ranges are helpful in determining a model that more thoroughly describes the magnetochemistry of the complex.

The temperature-dependent magnetic susceptibility plot (6–300 K) for [Fe(TPrP)(Cl)] (Figure 6) is characteristic of a high-spin iron(III) complex; the room temperature μ_{eff} value of 5.90 corresponds with the spin-only moment for a S = 5/2 center, and the zero-field splitting parameter (6.95 cm^{-1}) is typical for this class of compounds.[47] The coupling constant derived from _tting the magnetic data for [Fe(TPrP)(Cl)] implies that there is an antiferromagnetic magnetic exchange interaction $J\vec{S}_1 \cdot \vec{S}_2$ between iron centers of J = +0.17 cm^{-1}. The temperature-dependent magnetic susceptibility plot for [Fe(TEtP)(Cl)] shows similar high-spin iron(III) characteristics (assuming a zero-field splitting parameter identical to that found in the [Fe(TPrP)(Cl)] case), but is best described as having a magnetic exchange coupling constant about two times as large as that found in [Fe(TPrP)(Cl)].

As can be seen in Table 3, there is a relatively large difference between the intermolecular geometric parameters of [Fe(TPrP)(Cl)] and [Fe(TEtP)(Cl)]. Most importantly, the Fe…Fe separation in [Fe(TEtP)(Cl)] (5.60 Å) is much smaller than that found in [Fe(TPrP)(Cl)] (6.44 Å). Also, as can be seen in Figures 5a and 5b, the porphyrin overlap pattern is different for

these two complexes. Thus, there is apparently a correlation between proximity of the iron centers of the dimeric unit and magnitude of magnetic exchange for these two complexes; stronger magnetic interaction between the iron centers of [Fe(TEtP)(Cl)] is most likely due to the closer proximity of the magnetic centers within the dimeric unit.

Thus, magnetic exchange coupling is found to be sensitive to modest structural changes between porphyrin dimer geometries, and this exchange interaction must be included in any detailed analysis of the data. In fact, it was reported that, in [Fe(OEP)(2-MeHIm)]ClO_4,[45] consideration of this antiferromagnetic interaction was needed for a good fit with the experimental data. Similarly, a small but significant antiferromagnetic exchange between iron centers has been noted in [Fe(TPP)(Cl)] (J = +0.14 cm^{-1}),[46] [Fe(OEP)(Cl)] (J = +0.02 cm^{-1}),[46] and hemin chloride (J = +0.08 cm^{-1}).[47] It should be noted that these coupling parameters are determined assuming a mean field model $J\langle \vec{S} \rangle \cdot \vec{S}$ rather than a dimer-only coupling scheme $J\vec{S}_1 \cdot \vec{S}_2$, thus care must be taken in comparing the coupling strengths.

Summary

We have prepared a series of *meso*-(tetraalkylporphinato)iron chloride complexes (alkyl = ethyl, *n*-propyl and *n*-hexyl). Their molecular structures indicate that inter-ring interactions change with alteration of the alkyl group substitutions in the *meso* positions. Magnetic exchange couplings between iron centers of the dimers are in accord with the trends in structural inter-ring geometries.

Supplementary Material

Refer to Web version on PubMed Central for supplementary material.

Acknowledgments

We thank the National Institutes of Health for support of this research under Grant GM-38401 to WRS. Funds for the purchase of the FAST area detector diffractometer was provided through NIH Grant RR-06709 to the University of Notre Dame. We also thank the National Science Foundation for the purchase of the SQUID equipment under Grant DMR-9703732.

References

1. a) Kuhlbrant W, Wang DN, Fujiyoshi Y. Nature (London) 1994;367:614–621. [PubMed: 8107845] b) McDermott G, Prince SM, Freer AA, Hawthorn-Thwaite-Lawless AM, Papiz MZ, Cogdell RJ, Isaacs NW. Nature (London) 1995;374:517–521.
2. Deisenhofer, J.; Norris, JR., editors. The Photosynthetic Reaction Center. Vol. Vol. 2. New York: Academic Press; 1993.
3. Scheidt WR, Lee YJ. Struct. Bonding (Berlin) 1987;64:1–70.
4. a) Scheidt WR, Geiger DK, Lee YJ, Reed CA, Lang G. J. Am. Chem. Soc 1985;107:5693–5699. b) Chen B, Safo MK, Orosz RD, Reed CA, Debrunner PC, Scheidt WR. Inorg. Chem 1994;33:1319–1324.
5. a) Scheidt WR, Cheng B, Haller KJ, Mislankar A, Rae AD, Reddy KV, Song H, Orosz RD, Reed CA, Cukiernik F, Marchon JC. J. Am. Chem. Soc 1993;115:1181–1183. b) Scheidt WR, Brancato-Buentello KE, Song H, Reddy V, Cheng B. Inorg. Chem 1996;35:7500–7507. c) Brancato-Buentello KE, Kang SJ, Scheidt WR. J. Am. Chem. Soc 1997;119:2839–2846.
6. Brancato-Buentello KE, Scheidt WR. Angew. Chem., Int. Ed. Engl 1997;36:1456–1459.
7. Song Y, Haddad RE, Jia S-L, Hok S, Olmstead MM, Nurco DJ, Schore NE, Zhang J, Ma J-G, Smith KM, Gazeau S, Pécaut J, Marchon J-C, Medforth CJ, Shelnutt JA. J. Am. Chem. Soc 2005;127:1179–1192. [PubMed: 15669857]
8. Haddad RE, Gazeau S, Pécaut J, Marchon J-C, Medforth CJ, Shelnutt JA. J. Am. Chem. Soc 2003;125:1253–1268. [PubMed: 12553827]

9. Ikeue T, Ohgo Y, Nakamura M. Chem. Commun 2003:220–221.
10. Ikeue T, Ohgo Y, Saitoh T, Yamaguchi T, Nakamura M. Inorg. Chem 2001;40:3423–3434. [PubMed: 11421688]
11. Ikeue T, Ohgo Y, Uchida A, Nakamura M, Fujii H, Yokoyama M. Inorg. Chem 1999;38:1276–1281. [PubMed: 11670913]
12. Nakamura M, Ikeue T, Fujii H, Yoshimura T, Tajima K. Inorg. Chem 1998;37:2405–2414.
13. Nakamura M, Ikeue T, Fujii H, Yoshimura T. J. Am. Chem. Soc 1997;119:6284–6291.
14. Ikeue T, Ohgo Y, Saitoh T, Nakamura M, Fujii H, Yokoyama M. J. Am. Chem. Soc 2000;122:4046–4076.
15. Ema T, Senge MO, Nelson NY, Ogoshi H, Smith KM. Angew. Chem., Int. Ed. Engl 1994;33:1879–1881.
16. Gallucci JC, Swepston PN, Ibers JA. Acta Crystallogr., Sect. B 1982;38:2134–2139.
17. Kutzler FW, Swepston PN, Yellin ZB, Ellis DE, Ibers JA. J. Am. Chem. Soc 1983;105:2996–3004.
18. Newcomb TP, Godfrey MR, Hoffman BM, Ibers JA. J. Am. Chem. Soc 1989;111:7078–7084.
19. Jentzen, W.; Turowska-Tyrk, I.; Scheidt, WR.; Shelnutt, JA. Abstract of 210th ACS National Meeting; Inorganic Division, 531; 1995 Aug.
20. Nakamura M, Ikeue T, Fujii H, Yoshimura T. J. Am. Chem. Soc 1997;119:6284–6291.
21. Nakamura M, Ikeue T, Fujii H, Yoshimura T, Tajima K. Inorg. Chem 1998;37:2405–2414.
22. Wolowiec S, Latos-Grazynski L, Toronto D, Marchon JC. Inorg. Chem 1998;37:724–732.
23. Senge MO, Medforth CJ, Forsyth TP, Lee DA, Olmstead MM, Jentzen W, Pandey RK, Shelnutt JA, Smith KM. Inorg. Chem 1997;36:1149–1163. [PubMed: 11669682]
24. Meot-Ner M, Adler AD. J. Am. Chem. Soc 1975;97:5107–5111.
25. Song XZ, Jentzen W, Jia SL, Jaquinod L, Nurco DJ, Medforth CJ, Smith KM, Shelnutt JA. J. Am. Chem. Soc 1996;118:12975–12988.
26. DiMagno SG, Wersching AK, Ross ICR. J. Am. Chem. Soc 1995;117:8279–8280.
27. Mazzanti M, Marchon J-C, Shang M, Scheidt WR, Jia S, Shelnutt JA. J. Am. Chem. Soc 1997;119:12400–12401.
28. DiMagno SG, Williams RA, Therien MJ. J. Org. Chem 1994;59:6943–6948.
29. Neya S, Funasaki N. J. Heterocyclic Chem 1997;34:689–690.
30. Lindsey JS, Schreiman IC, Hsu HC, Kearney PC, Marguerettaz AM. J. Org. Chem 1987;52:827–836.
31. Adler AD, Longo FR, Kampas F, Kim J. J. Inorg. Nucl. Chem 1970;32:2443–2445.
32. The structure of [Fe(TPrP)(Cl)] has been reported earlier. The structure was determined at 298 K, with temperature effects considered, there are no significant differences. Ohgo Y, Ikeue T, Nakamura M. Acta Crystallogr., Sect. C 1999;C55:1817–1819.
33. Scheidt WR, Turowska-Tyrk I. Inorg. Chem 1994;33:1314–1318.
34. Sheldrick GM. Acta Crystallogr., Sect. A 1990;A46:467–473.
35. Sheldrick GM. Acta Crystallogr., Sect. A 2008;A64:112–122. [PubMed: 18156677]
36. The process is based on an adaptation of the DIFABS[37] logic to area detector geometry by Karaulov: Karaulov, A. I. Cardiff CF1 3TB, UK: School of Chemistry and Applied Chemistry, University of Wales, College of Cardiff; personal communication.
37. Walker NP, Stuart D. Acta Crystallogr., Sect. A 1983;A39:158–166.
38. Sutter TPG, Hambright P, Thorpe AN, Quoc N. Inorg. Chim. Acta 1992;195:131–132.
39. Selwood, PW. Magnetochemistry. New York: Interscience; 1956. Chapter 2.
40. Earnshaw, A. Introduction to Magnetochemistry. London: Academic; 1968. Chapter 1.
41. Scheidt WR, Finnegan M. Acta Crystallogr., Sect. C 1989;C45:1214–1216. [PubMed: 2604945]
42. Ernst J, Subramanian J, Fuhrhop J-HZ. Naturforsch 1977;32A:1129–1136.
43. Scheidt WR, Reed CA. Chem. Rev 1981;81:543–555.
44. a) Behere DV, Date SK, Mitra S. Chem. Phys. Lett 1979;68:544–548. b) Behere DV, Mitra S. Indian J. Chem 1980;19(A):505–507.
45. Gupta GP, Lang G, Scheidt WR, Geiger DK, Reed CA. J. Chem. Phys 1985;83:5945–5952.
46. Marathe VR, Mitra S. J. Chem. Phys 1983;78:915–920.

47. Richards PL, Caughey WS, Ebersacher H, Feher G, Malley MM. J. Chem. Phys 1967;47:1187–1888.

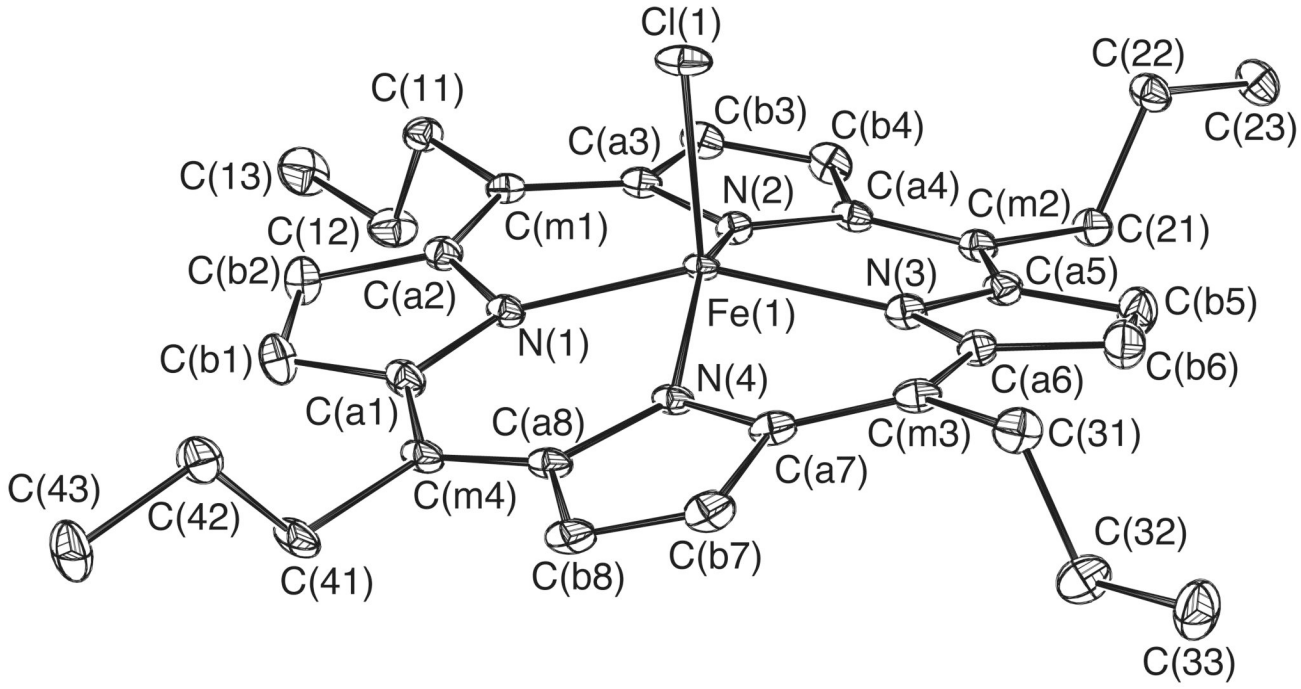

Figure 1.
ORTEP diagram of [Fe(TPrP)(Cl)]. Ellipsoids are drawn to illustrate 50% probability surfaces. Hydrogen atoms have been omitted for clarity.

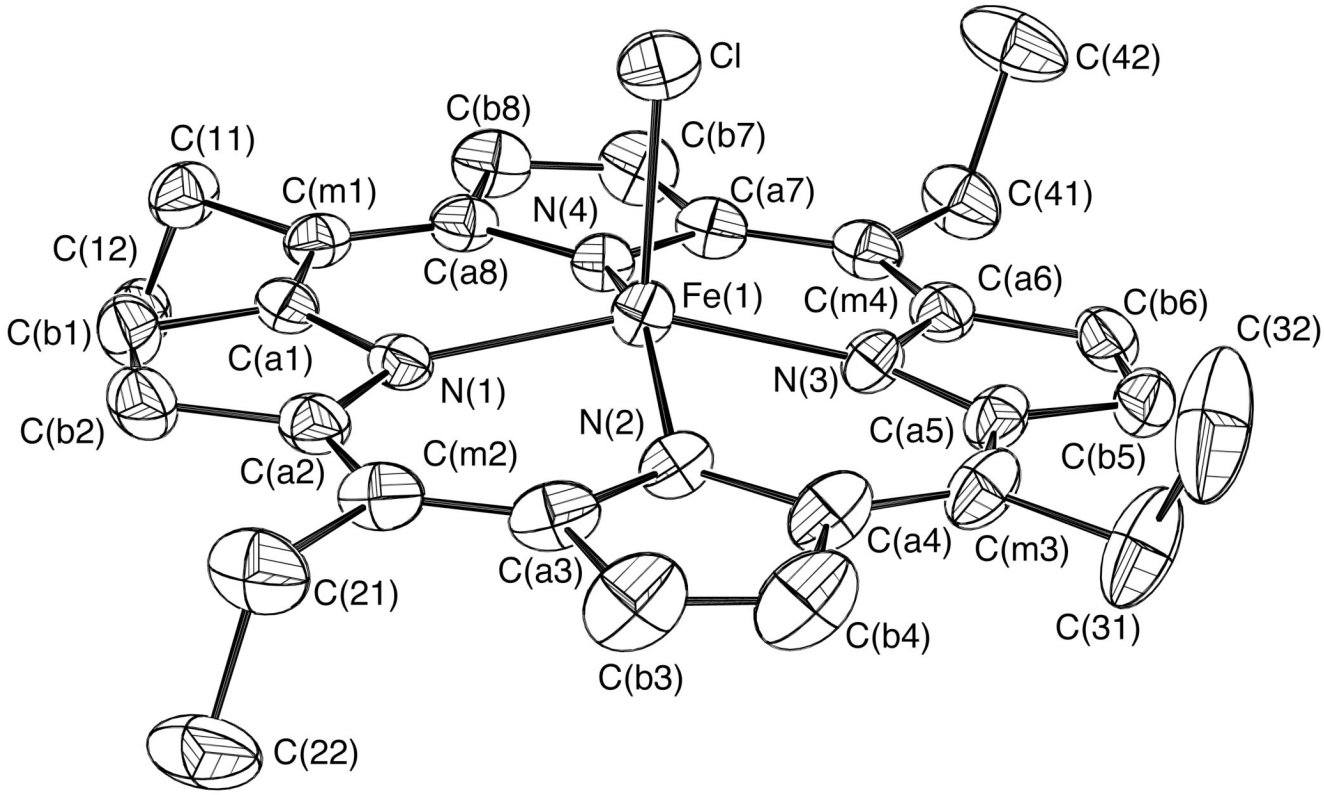

Figure 2.
ORTEP diagram of [Fe(TEtP)(Cl)]. Ellipsoids are drawn to illustrate 50% probability surfaces. Hydrogen atoms have been omitted for clarity.

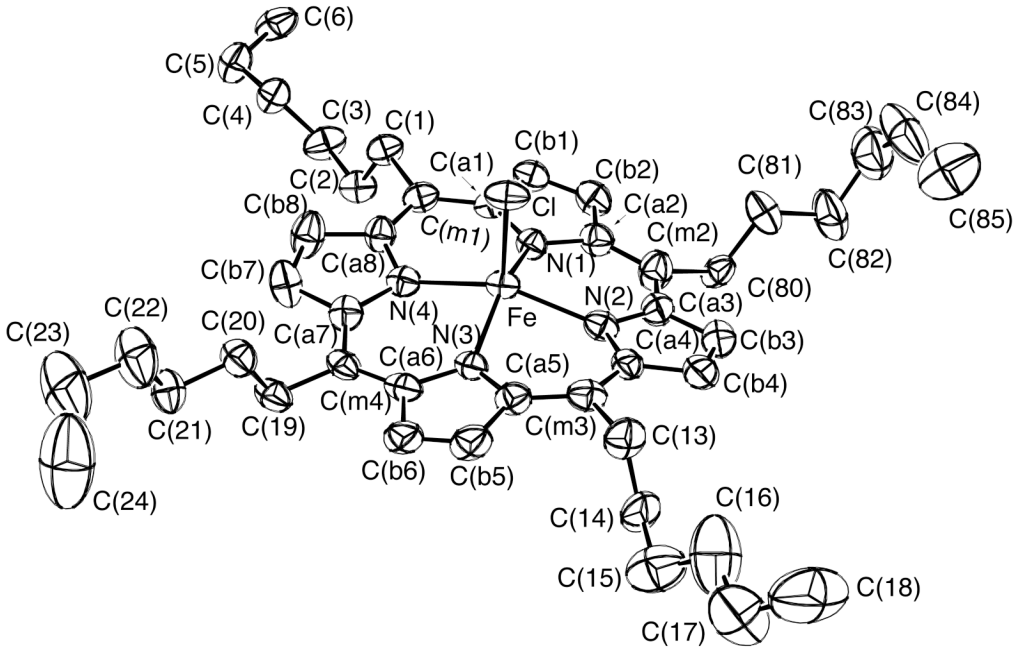

Figure 3.
ORTEP diagram of [Fe(THexP)(Cl)]. Ellipsoids are drawn to illustrate 50% probability surfaces. Hydrogen atoms have been omitted for clarity.

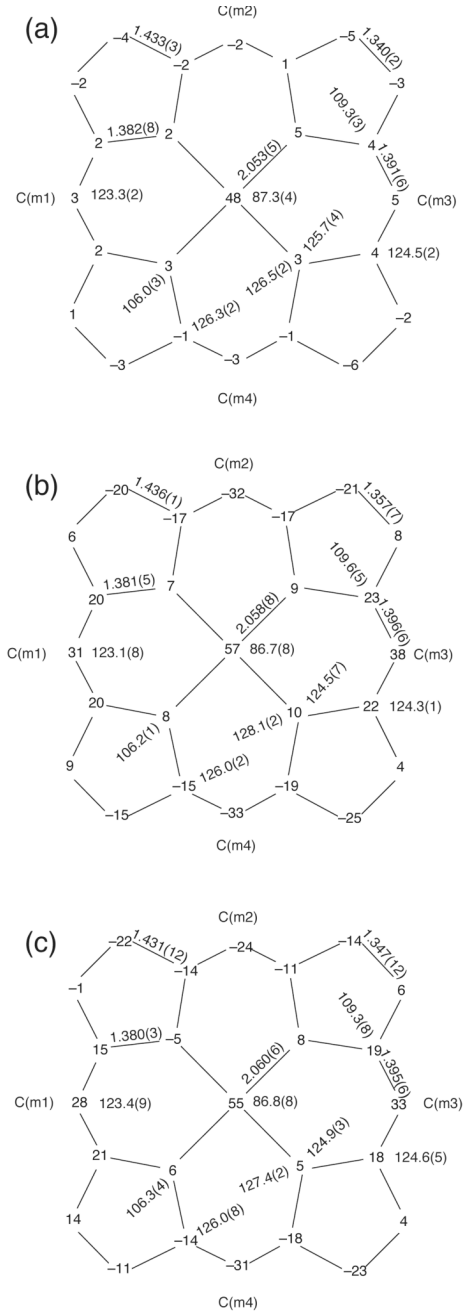

Figure 4.

Formal 24-atom mean-plane diagrams of (a) [Fe(TEtP)(Cl)], (b) [Fe(TPrP)(Cl)], and (c) [Fe (THexP)(Cl)]. The displacement of each atom from the 24-atom mean plane of the core is given in units of 0.01 Å. Also displayed are the averaged values of each type of bond distance and angle in the core. The number in parentheses is the standard deviation calculated on the assumption that all averaged values were drawn from the same population.

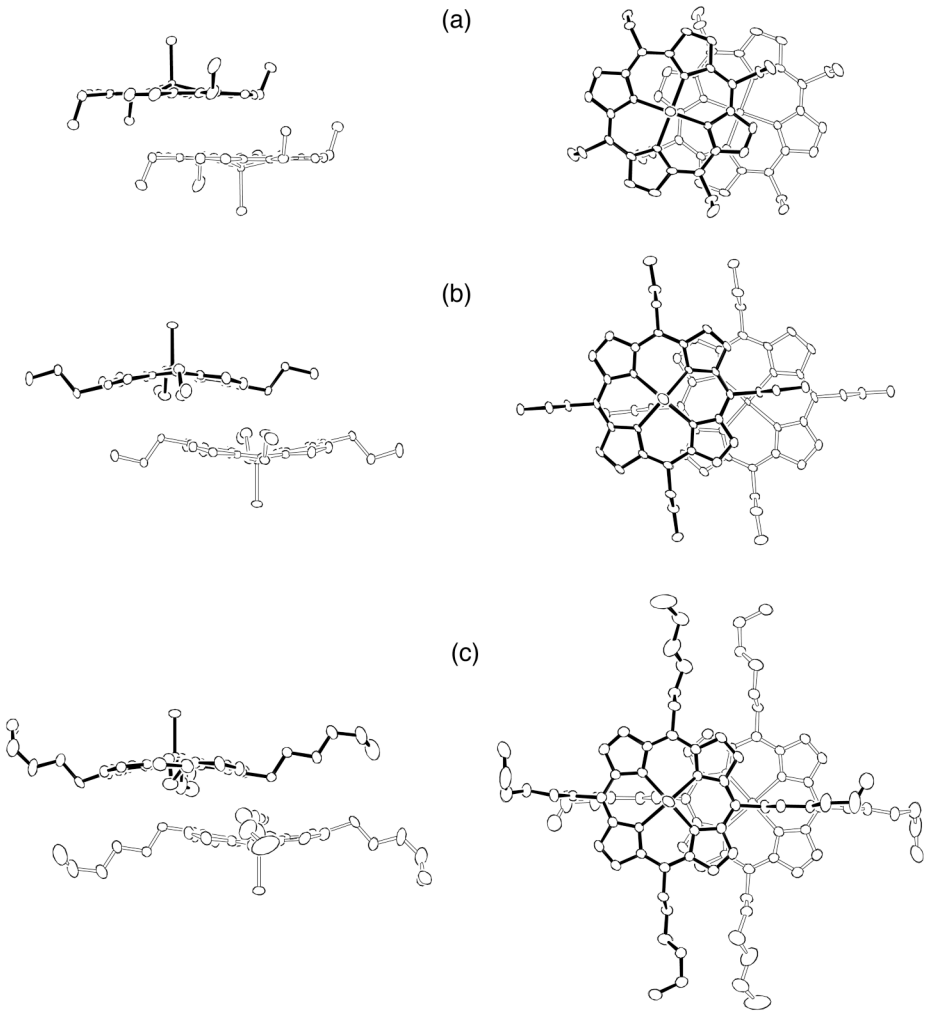

Figure 5.
Edge-views and top-views of the dimeric units of (a) [Fe(TEtP)(Cl)], (b) [Fe(TPrP)(Cl)], and (c) [Fe(THexP)(Cl)]. Ellipsoids are drawn to illustrate 30% probability surfaces for [Fe(TEtP)(Cl)], 65% probability surfaces for [Fe(TPrP)(Cl)], and 30% probability surfaces for [Fe(THexP)(Cl)].

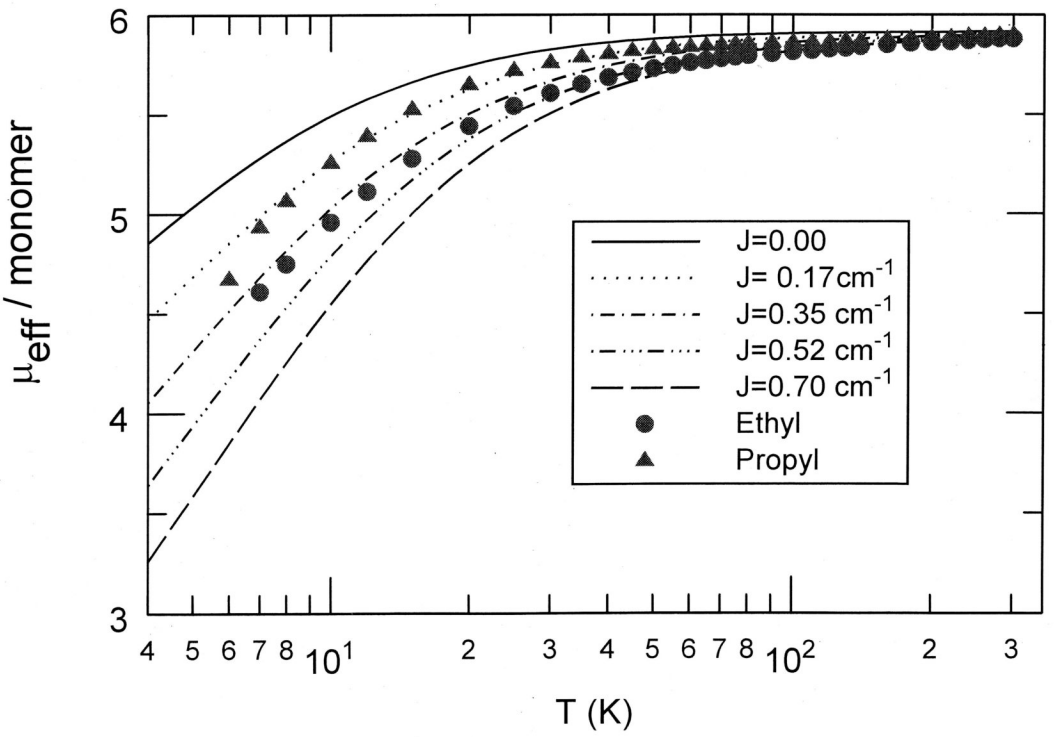

Figure 6.

Comparison of observed and calculated values of μ_{eff}/monomer vs T for (a) [Fe(TEtP)(Cl)] and (b) [Fe(TPrP)(Cl)]. The solid lines are model calculation with the parameters–axial zero-field splitting D = 6.95 cm^{-1}, antiferromagnetic coupling with J = +0.45 for (a) and J = +0.17 cm^{-1} for (b).

Table 1

Crystallographic details for [Fe(TalkylP)(Cl)] complexes.

Molecule	**[Fe(TEtP)(Cl)]**	**[Fe(TPrP)(Cl)]**	**[Fe(THexP)(Cl)]**
Formula	$C_{28}H_{28}ClFeN_4$	$C_{32}H_{36}ClFeN_4$	$C_{44}H_{60}ClFeN_4 \cdot 0.1CH_2Cl_2$
FW, amu	511.84	567.95	744.75
a, Å	10.1710(5)	13.040(2)	10.246(7)
b, Å	11.309(3)	15.221(2)	12.834(4)
c, Å	12.170(3)	14.6681(9)	17.420(15)
α, deg	91.774(9)	90	69.74(3)
β, deg	113.170(14)	109.997(11)	87.52(4)
γ, deg	112.149(9)	90	84.89(3)
V, Å^3	1165(4)	2735.9(7)	2140(2)
Crystal system	triclinic	monoclinic	triclinic
Space Group	$P\bar{1}$	$P2_1/n$	$P\bar{1}$
Z	2	4	2
D_c, g/cm^3	1.459	1.379	1.156
F(000)	534	1196	790
μ, mm^{-1}	0.787	0.678	0.448
Radiation ($\bar{\lambda}$, Å)	MoKα (0.71073)	MoKα (0.71073)	MoKα (0.71073)
Temperature, K	130(2)	130(2)	130(2)
R indices [I > 2σ(I)]	R_1 = 0.0884, wR_2 = 0.2073	R_1 = 0.0477, wR_2 = 0.1176	R_1 = 0.1024, wR_2 = 0.2659
R indices (all data)	R_1 = 0.1060, wR_2 = 0.2254	R_1 = 0.0556, wR_2 = 0.1235	R_1 = 0.1647, wR_2 = 0.3239
Goodness-of-fit on F^2	1.055	1.052	1.026

Table 2

Select bond distance(Å) and angles(°) for [Fe(TalkylP)(Cl)] complexes.

	[Fe(TEtP)(Cl)]	[Fe(TPrP)(Cl)]	[Fe(THexP)(Cl)]
A. Bond Lengths (Å)			
Fe(1)–N(1)	2.060(3)	2.063(1)	2.068(4)
Fe(1)–N(2)	2.052(3)	2.054(1)	2.063(5)
Fe(1)–N(3)	2.048(3)	2.055(1)	2.056(4)
Fe(1)–N(4)	2.051(3)	2.062(1)	2.054(5)
Fe(1)–Cl	2.2644(13)	2.2332(6)	2.2375(18)
B. Bond Angles (deg)			
N(1)–Fe(1)–N(2)	86.66(14)	86.30(6)	87.32(17)
N(1)–Fe(1)–N(4)	87.54(14)	86.88(6)	86.31(17)
N(2)–Fe(1)–N(3)	87.49(14)	87.16(6)	86.41(17)
N(3)–Fe(1)–N(4)	87.45(14)	86.50(6)	87.23(18)
N(1)–Fe(1)–N(3)	154.47(14)	152.24(6)	152.14(17)
N(2)–Fe(1)–N(4)	155.21(14)	152.31(6)	153.32(17)

Table 3

Summary of inter-ring geometries for [Fe(TalkylP)(Cl)] complexes.[a]

Complex	Fe···Fe	Ct···Ct[b]	M.P.S.[c]	L.S.[d]	Group	Δ[e]
[Fe(TEtP)(Cl)]	5.56	5.04	3.34	3.79	I	0.48
[Fe(TPrP)(Cl)]	6.44	5.64	3.66	4.29	W	0.57
[Fe(THexP)(Cl)]	6.36	5.77	3.64	4.48	W	0.55

[a]Values in Å.

[b]Ct is the center of the 24-atom porphyrin ring.

[c]The average mean plane separation for the two 24-atom cores of the dimer.

[d]The lateral shift between the two 24-atom cores of the dimer.

[e]The out-of-plane displacement relative to the 24-atom mean plane.

Table 4

Summary of inter-ring coupling for various iron dimers.[a]

Complex	Fe···Fe	M.P.S.[b]	L.S.[c]	J, cm^{-1}	ref.
[Fe(TPP)($B_{11}CH_{12}$)]·C_7H_8	5.49	3.83	3.67	+3.0	*d*
[Fe(OEP)(2-MeHIm)]ClO_4·CH_2Br_2	4.28	3.31	1.49	+0.85	*e*
[Fe(OEP)(2-MeHIm)]ClO_4·$CHCl_3$	4.60	3.42	2.15	+0.8	*e*
[Fe(TEtP)(Cl)]	5.56	3.34	3.79	+0.45	this work
[Fe(TPrP)(Cl)]	6.44	3.66	4.29	+0.17	this work

[a] Values in Å.

[b] The average mean plane separation for the two 24-atom cores of the dimer.

[c] The lateral shift between the two 24-atom cores of the dimer.

[d] *Inorg. Chem.* **1987**, *26*, 3022–3030. Sign adjusted to $+J\vec{S}_1 \cdot \vec{S}_2$

[e] *J. Chem. Phys.* **1985**, *83*, 5945–5952. Sign adjusted to $+J\vec{S}_1 \cdot \vec{S}_2$